Jin Zheng (Orcid ID: 0000-0002-3643-7314)

You Qinglong (Orcid ID: 0000-0002-5329-9697)

Mu Mu (Orcid ID: 0000-0002-6841-5611)

Sun Guodong (Orcid ID: 0000-0003-1495-6516)

Pepin Nick (Orcid ID: 0000-0001-6200-4937)

Fingerprints of anthropogenic influences on vegetation change over the Tibetan Plateau from an eco-hydrological diagnosis

Zheng Jin[1], Qinglong You[1, 2*], Mu Mu[1], Guodong Sun[3], Nick Pepin[4]

[1] Department of Atmospheric and Oceanic Sciences & Institute of Atmospheric Sciences, Fudan University, 200438, Shanghai, China;

[2] Innovation Center of Ocean and Atmosphere System, Zhuhai Fudan Innovation Research Institute, Zhuhai, 518057, China;

[3] State Key Laboratory of Numerical Modeling for Atmospheric Sciences and Geophysical Fluid Dynamics (LASG), Institute of Atmospheric Physics, Chinese Academy of Sciences, Beijing 100029, China;

[4] Department of Geography, University of Portsmouth, PO1 3HE, U.K.

This article has been accepted for publication and undergone full peer review but has not been through the copyediting, typesetting, pagination and proofreading process which may lead to differences between this version and the Version of Record. Please cite this article as doi: 10.1029/2020GL087842

* Corresponding author:

Prof. Qinglong You (qlyou@fudan.edu.cn or yqingl@126.com)

Department of Atmospheric and Oceanic Sciences & Institute of Atmospheric Sciences, Fudan University

Room 5002-1, Environmental Science Building, No.2005 Songhu Road, Yangpu 200438, Shanghai, China

Key Points:

- Climate change induced significant vegetation cover change has occurred in subregions of the Tibet plateau over the past three decades.
- A diagnose method linked the supply and demand for water and energy in land surface climate-vegetation system is utilized.
- Anthropogenic factor of vegetation browning has achieved obvious expansion in the past 30 years.

Abstract

Vegetation cover exerts a strong control on land-atmosphere interactions. To quantify the relative effects of external forcing (climate change) vs internal forcing (anthropogenic activity) on recent vegetation change over the Tibetan Plateau (TP), we apply an eco-hydrological diagnostic framework, developed from earlier work. We compare vegetation change during 1986-2015 based on NDVI (Normalized Difference Vegetation Index) data with changes in environmental conditions (European Centre for Medium-Range Weather Forecasts Reanalysis 5th-generation, ERA5). Results show that external forcing is the dominant factor behind significant vegetation change over the southeastern TP during 1986-2015. In the area with significant vegetation changing, 60.5%/41.5% of pixels have experienced a respective wetting/drying of climate, which in turn has supported greening/browning during 1986-2005/1996-2015. However, during the greening/browning transition in the latter period, the

proportion of internal forcing on browning increased from 5.62% to 19.4%, indicating that anthropogenic factors are playing an increasingly role on impacting vegetation change in recent decades.

Plain Language Summary

In climate systems, vegetation is a layer that situated at the border of the atmosphere and land surface, controlling the exchange of water and energy. However, vegetation is fragile in cold and arid region like the Tibetan Plateau, and can easily be influenced both by climate change (sunlight, rainfall, temperature, etc.) and human activities (land use, grazing, farming, etc.). In order to figure out to what extent the vegetation is affected by climate change or human activities, we combine historical land surface climate data and satellite-observed vegetation data to investigate the theoretical inducement of climate and human factors. Results show that in the areas with significant vegetation changing (mostly southeastern Tibetan plateau), climate change is dominant control of vegetation change in the past three decades. However, the human factor has significantly increased in importance over recent decades.

1 Introduction

Energy and water transfers between the land surface and atmosphere are critical parts of climate systems, particularly over the Tibetan Plateau (TP). The elevated surface is a powerful "heat pump" to the global atmosphere [Ye, 1981; Yanai *et al*., 1992] and any change in that heat source can affect climate throughout the Northern Hemisphere [Li *et al*., 2017; Li *et al*., 2019]. Since transpiration from vegetation controls the ratio of sensible to latent heat given a fixed input of solar radiation [Thom, 1972], vegetation change on TP will affect the

strength of the "heat pump" by reducing/increasing the surface sensible/latent heat flux. Through dynamic forcing which can change the regional circulation pattern, sensible heat from the land surface can also influence summer rainfall over the whole of China [Zuo *et al*., 2011; Duan *et al*., 2012]. The TP is also recognized as the "Asian water tower", playing an important role in both regional and global water cycles due to high storage of freshwater [Qiu, 2008; Xu *et al*., 2008]. The regional water cycle over the TP can also be affected by changes in transpiration, soil moisture, and ground runoff associated with vegetation change [Kleidon and Heimann, 2000; Moore *et al*., 2007; Seneviratne *et al*., 2010].

Climate change will influence vegetation composition and health [Overpeck *et al*., 1990; Theurillat and Guisan, 2001], and local anthropogenic activities also can act directly, e.g. deforestation and changing land-use [Piao *et al*., 2003; Wang *et al*., 2008; Wang and Hejazi, 2011]. There are large-scale ecological protection projects within the region [Ouyang *et al*., 2016; Xu *et al*., 2017; Bryan *et al*., 2018]. In particular, the impacts of anthropogenic vegetation restoration on the conservation of water resources over the TP deserves further research. Since energy and water transfers between land surface and atmosphere are critical parts of climate systems, approaches to quantify the role of various forcing factors on vegetation change are required to further understand the role of vegetation in environmental change.

Based on an eco-hydrological approach, a diagnostic method to quantify the role of vegetation in transferring energy and moisture originated from the pioneering work of Budyko [1974]. This approach later developed a dryness index [Tomer and Schilling, 2009; Renner *et al*., 2012] and more recent work has applied the eco-hydrological conceptual model to understanding of regional scale vegetation dynamics through merging remote sensing with

reanalysis data. Vegetation change is quantified in an eco-hydrological state related to water and energy transits [Cai *et al.*, 2015; Cai *et al.*, 2016]. The increase/decrease of vegetation would result in increase/decrease of water and energy demand, which lead to changes of eco-hydrological state. Because of restricted data, the first eco-hydrological diagnoses of vegetation dynamics over the TP [Cai *et al.*, 2015] and in south America [Cai *et al.*, 2016] were limited to comparisons between two periods (1982-1993 and 1994-2006). Recent updated data provides an extension of nine years (2007-2015), allowing study of vegetation changes and eco-hydrological attributions for a longer period. In previous work [Cai *et al.*, 2015; Cai *et al.*, 2016], significant change was defined by differences in relative amplitude (exceeding one standard deviation of water or energy excess). However, as vegetation is at the core of the water-energy link in the eco-hydrological diagnostic framework, the amplitude of vegetation change itself is a more efficient indicator of significant change in eco-hydrological status. Therefore, our study focuses on sub-regions where the absolute amplitude of vegetation change is large compared to other parts of the TP.

2 Data and Methodology

2.1 Temporal scale settings and the boundary of TP

According to measurements of soil respiration in the alpine meadows of the TP [Li *et al.*, 2019], the growing season in most of the TP starts in May and ends in September, which is defined in this study. Most areas in the central and southeastern TP have mean NDVI over 0.2 during these five months. The choice of long-term average period is critical for eco-hydrological diagnostics [Milne *et al.*, 2002], because both climate and vegetation change over

time. We require ten years to define a reasonable period, and thus compare three periods: 1986-1995, 1996-2005 and 2006-2015. The average values of all variables in the growing season are used.

The boundary of the TP is determined using 2,500-meter elevation contour, combined with national boundaries [Zhang, 2019]. The whole TP is represented by 4858 grid points.

2.2 Remote sensing vegetation cover data

NDVI is widely used to quantify land surface vegetation. The Global Inventory Monitoring and Modeling Studies (GIMMS) NDVI 3rd-generation gridded dataset has a horizontal spatial resolution of 1/12° and a half-monthly interval [Tucker *et al*., 2005]. The dataset spans from July 1981 to December 2015 (https://ecocast.arc.nasa.gov/data/pub/gimms/). The observations are obtained from Advanced Very High Resolution Radiometer (AVHRR), placed on the National Oceanic and Atmospheric Administration (NOAA) satellite series (https://www.noaa.gov/). In this study, the GIMMS NDVI data were resampled to a horizontal spatial resolution of 1/4° and a monthly interval to make them comparable with the climate data.

2.3 Surface climate data

ERA5 is the 5th-generation reanalysis of the European Centre for Medium-Range Weather Forecasts (ECMWF). Currently available from 1979 to present, it has officially replaced ERA-Interim [Hans *et al*., 2019]. In our study, evaporation, total precipitation, surface net solar radiation, and surface net thermal radiation are used (accessible at: https://doi.org/10.24381/cds.f17050d7). Monthly means are gridded at 1/4° horizontal

resolution. Totally, ERA5 can capture the climate change representability of above-mentioned variables over the TP.

2.4 Eco-hydrological diagnostic method

At the scale-appropriate to land surface ecosystems (each grid box has an area of approximately 120 km^2), there are two simple balance equations in water and energy respectively:

$$P = Ro + E \quad (1)$$

$$N = H + E \quad (2)$$

where P is total precipitation, Ro is runoff (surface and underground flow), E is evapotranspiration, N is surface net radiation, H is the surface sensible heat flux. Evapotranspiration occurs in both equations since it is both a flux of water and energy. When E is calculated in terms of energy (latent heat flux), water amount is transformed to energy flux units via multiplying by 2.5×10^6 J kg^{-1} (mm/day to $J\cdot m^{-2}$/day). Here the ground water and energy storage are ignored, because 10-year averages are applied to all variables, variations in long-term water and energy storage are negligible. The portion of water and energy supply not being used by the vegetation can be respectively defined as relative excess water W and relative excess energy U [Milne *et al.*, 2002]:

$$W = Ro / P \quad (3)$$

$$U = H / N \quad (4)$$

Substituting equations (1) and (2) for R_0 and H respectively, we obtain:

$$W = 1 - E / P \quad (5)$$

$$U = 1 - E / N \quad (6)$$

The ratio of energy to water supply is defined as the drought index [Budyko and Miller, 1974]:

$$D = N / P \quad (7)$$

Here the unit of P is transformed to the equivalent energy flux as in the above-mentioned transformation of E. Interpreting the energy supply N as the leading energy input for evaporation, the drought index D can separate energy limited regimes (D<1, wet) from water limited regimes (D>1, dry). Combining W and U, we can introduce the (W, U)-diagram (**Figure 1a**). The Schreiber curve in Figure 1a is the empirical formula of an ideal rainfall-runoff chain [Fraedrich, 2010]. Eco-hydrological status in (W, U) coordinates is based on long-term averages of climate variables [Milne *et al*., 2002]. Once the average (W, U) status changes from one period to another, the difference can be calculated and represented as a trajectory. Based on the direction of this trajectory, there are four types of eco-hydrological change: ($W\downarrow$, $U\uparrow$) indicates external forcing since energy is increasing and water supply is decreasing which occurs when an area becomes drier; ($W\uparrow$, $U\downarrow$) also indicates external forcing which occurs when an area becomes wetter (the opposite). However, the other two changes: ($W\uparrow$, $U\uparrow$) indicates an internal process associated with decreasing vegetation, whereas ($W\downarrow$, $U\downarrow$) indicates an internal process with increasing vegetation. Our definition of internal vs external forcing is based on the influence of vegetation change on surface water and energy flux. When the change

of (*W*, *U*) is mainly controlled by vegetation, there would be consequences as (*W*↑, *U*↑) and (*W*↓, *U*↓). Otherwise the change of (*W*, *U*) is mainly controlled by the climate change, which is external forcing (external of biosystem).

3 Results

3.1 Inconsistent changes in vegetation over time

The average spatial pattern of growing season means NDVI in 1986-2015 is shown in **Figure 1b**. Yellow/green areas indicate lower/higher. The highest values are generally in the south and east of the plateau. Correspondingly, the geographical patterns of eco-hydrological status (*W*, *U*) are showed (**Figure 1c, d**). Black boundaries (**Figure 1e-h**) encircle areas where the changes in NDVI are inconsistent and differ between sub-periods. Significant contrast between periods is defined as $|C_{S1} - C_{S2}| > 0.03$, where C_{S1} is the mean NDVI between 1986-1995 and 1996-2005: Stage 1), C_{S2} is the mean NDVI between1996-2005 and 2006-2015: Stage 2).

The vegetation change (inside the black boundaries) can be divided into two types; type 1 (T1) in which the NDVI decreases in Stage 1 and increases in Stage 2, and type 2 (T2) in which the NDVI increases in Stage 1 and decreases in Stage 2. There are 112 (2.3%) and 284 (5.8%) grid points belonging to T1 and T2, respectively. T1grid points are dispersed across the plateau, including areas to the south of Qinghai lake (37°N, 100°E) (**Figure 1e, f**) and in the south of the Himalayas. T1 areas thus show wide range of environmental backgrounds such as latitude, altitude and exposure to the summer monsoon. On the other hand, T2 grid points

appear to be clustered in the southeast of the TP where there has been a significance change from greening (increased NDVI) in Stage 1 to browning (decreased NDVI) in Stage 2.

3.2 Drought status background and eco-hydrological attribution

In a similar way to vegetation change we also examine change in the climate forcing including the drought index. Based on 30 year climatology (1985-2016) (**Figure 2a**) there are three extremely arid regions over the TP where the drought index is mostly above D=5: the Pamirs plateau (35°N~39°N, 68°E~74°E), the Changtang region (28°N~36°N, 76°E~88°E) and the Qaidam basin (36°N~39°N, 89°E~98°E). Even in the growing season, these regions are rarely covered by extensive vegetation. The drought index changes in Stage 1 (**Figure 2b**) and Stage 2 (**Figure 2c**) show wetting (Stage 1) and drying (Stage 2) tendencies over much of the mid and southeast TP corresponding with the increased/decreased NDVI in the same region (T2).

We use the eco-hydrological diagnostic method and examine how water and energy excess have changed in the 284 grid points representing the T2 area. From Stage 1 to Stage 2, the number of grid points with ($W\uparrow$, $U\downarrow$) declined from 172 to 19 (**Figure 3**), while the ($W\downarrow$, $U\uparrow$) grid points increased from 5 to 118. Thus, the greening in Stage 1 is mostly correlated with wetter climate forcing, 60.5% of the greened area experiencing an increase in water excess and decrease in energy excess ($W\uparrow$, $U\downarrow$) (**Table 1**). Browning in Stage 2 is correlated with dry climate forcing, 41.5% of the area experiencing reduced water and increased energy ($W\downarrow$, $U\uparrow$). The dominating eco-hydrological forcing from Stage 1 to Stage 2 is ($W\uparrow$, $U\downarrow$) to ($W\downarrow$, $U\uparrow$), which covers 32.7% of all status conversions. It is worth noting that although the anthropogenic

browning process ($W\uparrow$, $U\uparrow$) possesses the least proportion, it expands from 5.62% to 19.4% between the two stages.

Drought index changes are numerically much larger in dry regions, so defining D=1 as the threshold between wet and dry conditions, we derived six drought change types (**Figure 2d, e**). The dominance of the climate (external) forcing in accounting for greening and browning is also supported by changes in the drought index. Examining the drought status background of T2 grid points, 225 grid points (60 W→W, 123 D→W, 42 D→W while crossing D=1) show wetting tendencies in Stage 1. By Stage 2, 160 grid points show drying tendencies. In Stage 1, 42 grid points crossed the wet/dry threshold, changing from arid to humid. In Stage 2, 28 grid points changed from humid to arid. This indicates that the spatial extent of wetting in Stage 1 is greater than the drying in Stage 2.

3.3 Typical trajectories of eco-hydrological status

We display typical trajectories of eco-hydrological status for T1 areas (**Figure 4a**) and T2 areas (**Figure 4b**) on the diagram. In theory, every grid point should have a trajectory from the first period (1986-1995) to the last period (2006-2015). However, some changes are too small to be visible on the diagram. Any change in water or energy excess between the two periods below 0.05 in T1 areas, and 0.08 in T2 areas is therefore ignored. There are 28/56 plotted trajectories in T1/T2 areas respectively.

The trajectories in T1 areas are mostly horizontal (**Figure 4a**), in other words, they are W induced. The NDVI decreased in Stage 1 while W increased. In Stage 2 NDVI increased but W continued to increase. T1 grid points are widely dispersed in different regions over the TP

and these trajectories are not conforming to an individual phenomenon. In T2 areas on the other hand (**Figure 4b**), the trajectories of Stage 1 and Stage 2 form acute angles with gray dots at the vertices. Unlike T1 areas, the terminal status of (*W*, *U*) (black dots) in T2 areas tends to stay near the initial status (hollow circles). This means that water and energy changes in Stage 1 are often reversed in Stage 2. These typical trajectories provide detailed information about eco-hydrological diagnose, including the ratio of *W* to *U*, the amplitude of change, the diagnostic status presented by coordinate position, and NDVI tendency. The results indicate that, in spatial consistent and changing significant area (T2 area), the eco-hydrological diagnose framework has a satisfied adaptability, which shows the vegetation change tendencies practically agreed with the directions of trajectory.

4 Conclusions and Discussions

Our study has revealed the extent to which inter-decadal vegetation changes over the southeast TP are driven by climate forcing. As we focused on the absolute amplitude of growing season NDVI change, the eco-hydrological diagnostic approach is different to that of *Cai et al.* [2015]. We have also expanded the earlier approach by defining regions exceeding an agreed NDVI change threshold, utilizing growing season, and dividing contrastive types for NDVI change trends. Other recent studies claimed that changes in NDVI are positively correlated with regional precipitation changes [Sun *et al.*, 2019], and that the precipitation-evapotranspiration water balance is a critical control on vegetation evolution [Liu *et al.*, 2019]. Our results also show that significant NDVI change is often correlated with climate forcing over the past three decades, agreeing with such studies. At the same time, faster urbanization [Tang *et al.*, 2017] and grazing pressure increase over the southeastern plateau region [Hafner

et al., 2012] were revealed in recent decades. Further, we also provide evidences for anthropogenic influence increase, including normalized human activity pressure index, land use pattern and socioeconomic statistics (not shown). Our method acknowledges that both climate forcing and anthropogenic activity simultaneously influence vegetation change, and that the latter, although remaining relatively small in comparison with dominant climate forcing, anthropogenic influence has increased in the later part of our analysis period.

When considering future application of the eco-hydrological diagnostic method elsewhere, we would urge caution in some circumstances. In desert regions with minimal vegetation, upward latent heat flux is not primarily controlled by vegetation, and thus an increase/decrease of vegetation in such regions may not systematically change the ratio of sensible/latent heat, making the method unreliable. NDVI itself in such regions can also respond to variance in other factors such as snow cover. In addition, although ERA5 is widely respected at representing environmental conditions, the diagnostic approach is only as reliable as the data which goes into it.

Acknowledgments

This study is supported by National Key R&D Program of China (2017YFA0603804) and National Natural Science Foundation of China (41971072, 41771069, 91937302 and 41911530187). The NDVI data were obtained from https://ecocast.arc.nasa.gov/data/pub/gimms/3g.v1/. The climate data were obtained from https://doi.org/10.24381/cds.f17050d7. We are very grateful to the reviewers for their constructive comments and thoughtful suggestions. Lastly, we would like to thank Zhizhen Xu, Fangying Wu and Liucheng Shen for their discussions and data collection.

References

Bryan, B. A., Gao, L., Ye, Y., Sun, X., Connor, J. D., Crossman, N. D., et al. (2018). China's response to a national land-system sustainability emergency. *Nature, 559*(7713), 193-204. https://doi.org/10.1038/s41586-018-0280-2

Budyko, M. I., & Miller, D. H. (1974). *Climate and life* (Vol. 508): Academic press New York.

Cai, D., Fraedrich, K., Sielmann, F., Guan, Y., & Guo, S. (2016). Land-Cover Characterization and Aridity Changes of South America (1982–2006): An Attribution by Ecohydrological Diagnostics . *Journal of Climate, 29*(22), 8175-8189. https://doi.org/10.1175/JCLI-D-16-0024.1

Cai, D., Fraedrich, K., Sielmann, F., Zhang, L., Zhu, X., Guo, S., & Guan, Y. (2015). Vegetation dynamics on the Tibetan Plateau (1982–2006): An attribution by ecohydrological diagnostics. *Journal of Climate, 28*(11), 4576-4584. https://doi.org/10.1175/JCLI-D-14-00692.1

Duan, A., Wang, M., Lei, Y., & Cui, Y. (2013). Trends in summer rainfall over China associated with the Tibetan Plateau sensible heat source during 1980–2008. *Journal of Climate, 26*(1), 261-275. https://doi.org/10.1175/JCLI-D-11-00669.1

Fraedrich, K. (2009). A Parsimonious Stochastic Water Reservoir: Schreiber's 1904 Equation. *Journal of Hydrometeorology, 11*(2), 575-578. https://doi.org/10.1175/2009JHM1179.1

Hans, H., Bell, W., Berrisford, P., Andras, H., Muñoz-Sabater, J., Nicolas, J., et al. (2019). Global reanalysis: goodbye ERA-Interim, hello ERA5. *ECMWF Newsletter, 159,* 17-24. https://doi.org/10.21957/vf291hehd7

Hafner, S., Sebastian, U., Elke, S., Becker, L., Xu, X. L., Li, X. G., et al. (2012). Effect of grazing on carbon stocks and assimilate partitioning in a Tibetan montane pasture revealed by $^{13}CO_2$ pulse labeling. *Global Change Biology, 18(2), 528-538*. https://doi.org/10.1111/j.1365-2486.2011.02557.x

Kleidon, A., & Heimann, M. (2000). Assessing the role of deep rooted vegetation in the climate system with model simulations: mechanism, comparison to observations and implications for Amazonian deforestation. *Climate Dynamics, 16*(2), 183-199. https://doi.org/10.1007/s003820050012

Li, J., Zheng, F., Sun, C., Feng, J., & Wang, J. (2019). Pathways of Influence of the Northern Hemisphere Mid-high Latitudes on East Asian Climate: A Review. *Advances in Atmospheric Sciences, 36*(9), 902-921. https://doi.org/10.1007/s00376-019-8236-5

Li, Y., Ding, Y., & Li, W. (2017). Interdecadal variability of the Afro-Asian summer monsoon system.

Advances in Atmospheric Sciences, 34(7), 833-846. https://doi.org/10.1007/s00376-017-6247-7

Li, Z., Gao, J., Wen, L., Zou, C., Feng, C., Li, D., & Xu, D. (2019). Dynamics of Soil Respiration in Alpine Wetland Meadows Exposed to Different Levels of Degradation in the Qinghai-Tibet Plateau, China. *Scientific Reports, 9*(1), 7469-7469. https://www.ncbi.nlm.nih.gov/pubmed/31097739

Liu, L., Niu, Q., Heng, J., Li, H., & Xu, Z. (2019). Transition Characteristics of the Dry-Wet Regime and Vegetation Dynamic Responses over the Yarlung Zangbo River Basin, Southeast Qinghai-Tibet Plateau. *Remote Sensing, 11*(10), 1254 .

Milne, B. T., Gupta, V. K., & Restrepo, C. (2002). A scale invariant coupling of plants, water, energy, and terrain. *Écoscience, 9*(2), 191-199. https://doi.org/10.1080/11956860.2002.11682705

Moore, N., Arima, E., Walker, R., & Ramos da Silva, R. (2007). Uncertainty and the changing hydroclimatology of the Amazon. *Geophysical Research Letters, 34*(14), L14707. https://doi.org/10.1029/2007GL030157

Ouyang, Z., Zheng, H., Xiao, Y., Polasky, S., Liu, J., Xu, W., et al. (2016). Improvements in ecosystem services from investments in natural capital. *Science, 352*(6292), 1455. http://science.sciencemag.org/content/352/6292/1455.abstract

Overpeck, J. T., Rind, D., & Goldberg, R. (1990). Climate-induced changes in forest disturbance and vegetation. *Nature, 343*(6253), 51-53. https://doi.org/10.1038/343051a0

Piao, S., Fang, J., Zhou, L., Guo, Q., Henderson, M., Ji, W., et al. (2003). Interannual variations of monthly and seasonal normalized difference vegetation index (NDVI) in China from 1982 to 1999. *Journal of Geophysical Research: Atmospheres, 108*(D14), 4401. https://doi.org/10.1029/2002JD002848

Qiu, J. (2008). China: The third pole. *Nature, 454*(7203), 393-396. https://doi.org/10.1038/454393a

Renner, M., & Bernhofer, C. (2012). Applying simple water-energy balance frameworks to predict the climate sensitivity of streamflow over the continental United States. *Hydrology and Earth System Sciences, 16*(8), 2531-2546. https://doi.org/10.5194/hess-16-2531-2012

Seneviratne, S. I., Corti, T., Davin, E. L., Hirschi, M., Jaeger, E. B., Lehner, I., et al. (2010). Investigating soil moisture–climate interactions in a changing climate: A review. *Earth-Science Reviews, 99*(3), 125-161. http://www.sciencedirect.com/science/article/pii/S0012825210000139

Sun, W., Wang, Y., Fu, Y. H., Xue, B., Wang, G., Yu, J., et al. (2019). Spatial heterogeneity of changes in vegetation growth and their driving forces based on satellite observations of the Yarlung Zangbo

River Basin in the Tibetan Plateau. *Journal of Hydrology, 574*, 324-332. http://www.sciencedirect.com/science/article/pii/S0022169419303841

Tang, W., Zhou, T. C,. Sun, J., Li, Y. R. & Li, W. P. (2017). Accelerated urban expansion in Lhasa city and the implications for sustainable development in a Plateau City. *Sustainability, 9(9), 1499.* https://doi.org/10.3390/su9091499

Theurillat, J.-P., & Guisan, A. (2001). Potential Impact of Climate Change on Vegetation in the European Alps: A Review. *Climatic Change, 50*(1), 77-109. https://doi.org/10.1023/A:1010632015572

Thom, A. S. (1972). Momentum, mass and heat exchange of vegetation. *Quarterly Journal of the Royal Meteorological Society, 98*(415), 124-134. https://doi.org/10.1002/qj.49709841510

Tomer, M. D., & Schilling, K. E. (2009). A simple approach to distinguish land-use and climate-change effects on watershed hydrology. *Journal of Hydrology, 376*(1), 24-33. http://www.sciencedirect.com/science/article/pii/S002216940900403X

Tucker, C. J., Pinzon, J. E., Brown, M. E., Slayback, D. A., Pak, E. W., Mahoney, R., et al. (2005). An extended AVHRR 8-km NDVI dataset compatible with MODIS and SPOT vegetation NDVI data. *International Journal of Remote Sensing, 26*(20), 4485-4498. https://doi.org/10.1080/01431160500168686

Wang, D., & Hejazi, M. (2011). Quantifying the relative contribution of the climate and direct human impacts on mean annual streamflow in the contiguous United States. *Water Resources Research, 47*(10), W00J12. https://doi.org/10.1029/2010WR010283

Wang, X., Zheng, D., & Shen, Y. (2008). Land use change and its driving forces on the Tibetan Plateau during 1990–2000. *CATENA, 72*(1), 56-66. http://www.sciencedirect.com/science/article/pii/S0341816207000628

Xu, W., Xiao, Y., Zhang, J., Yang, W., Zhang, L., Hull, V., et al. (2017). Strengthening protected areas for biodiversity and ecosystem services in China. *Proceedings of the National Academy of Sciences, 114*(7), 1601. http://www.pnas.org/content/114/7/1601.abstract

Xu, X., Lu, C., Shi, X., & Gao, S. (2008). World water tower: An atmospheric perspective. *Geophysical Research Letters, 35*(20), L20815. https://doi.org/10.1029/2008GL035867

Yanai, M., Li, C., & Song, Z. (1992). Seasonal heating of the Tibetan Plateau and its effects on the evolution of the Asian summer monsoon. *Journal of the Meteorological Society of Japan, 70*(1B), 319-351.

https://doi.org/10.2151/jmsj1965.70.1B_319

Ye, D. (1981). Some Characteristics of the Summer Circulation Over the Qinghai-Xizang (Tibet) Plateau and Its Neighborhood. *Bulletin of the American Meteorological Society, 62*(1), 14-19. https://doi.org/10.1175/1520-0477(1981)062<0014:SCOTSC>2.0.CO;2

Zhang, G. (2019). *Dataset of river basins map over the TP (2016)*. Retrieved from: http://dx.doi.org10.11888/BaseGeography.tpe.249465.file

Zuo, Z., Zhang, R., & Zhao, P. (2011). The relation of vegetation over the Tibetan Plateau to rainfall in China during the boreal summer. *Climate Dynamics*, 36(5), 1207-1219. https://doi.org/10.1007/s00382-010-0863-6

Table 1. Percentages (%) of grid cells in area T2 with various changes in eco-hydrological diagnostic status from Stage 1 to Stage 2. All figures are the proportion of the 284 T2 grid points. Bold numbers are the conversion percentages from external to internal or vice versa. Italic numbers on the diagonal show the percentages of cells remaining unchanged. The numbers are rounded to 1 significant figure.

Stage 2	Stage 1				
	($W\downarrow$, $U\uparrow$)	($W\uparrow$, $U\uparrow$)	($W\downarrow$, $U\downarrow$)	($W\uparrow$, $U\downarrow$)	sum
($W\downarrow$, $U\uparrow$)	*0*	**0.3**	**8.4**	32.7	41.5
($W\uparrow$, $U\uparrow$)	**0.3**	*0*	16.2	**2.8**	19.4
($W\downarrow$, $U\downarrow$)	**0**	4.5	*3.1*	**24.6**	32.3
($W\uparrow$, $U\downarrow$)	1.4	**0.7**	**4.2**	*0.3*	6.6
sum	1.7	5.6	32.0	60.5	*3.5*

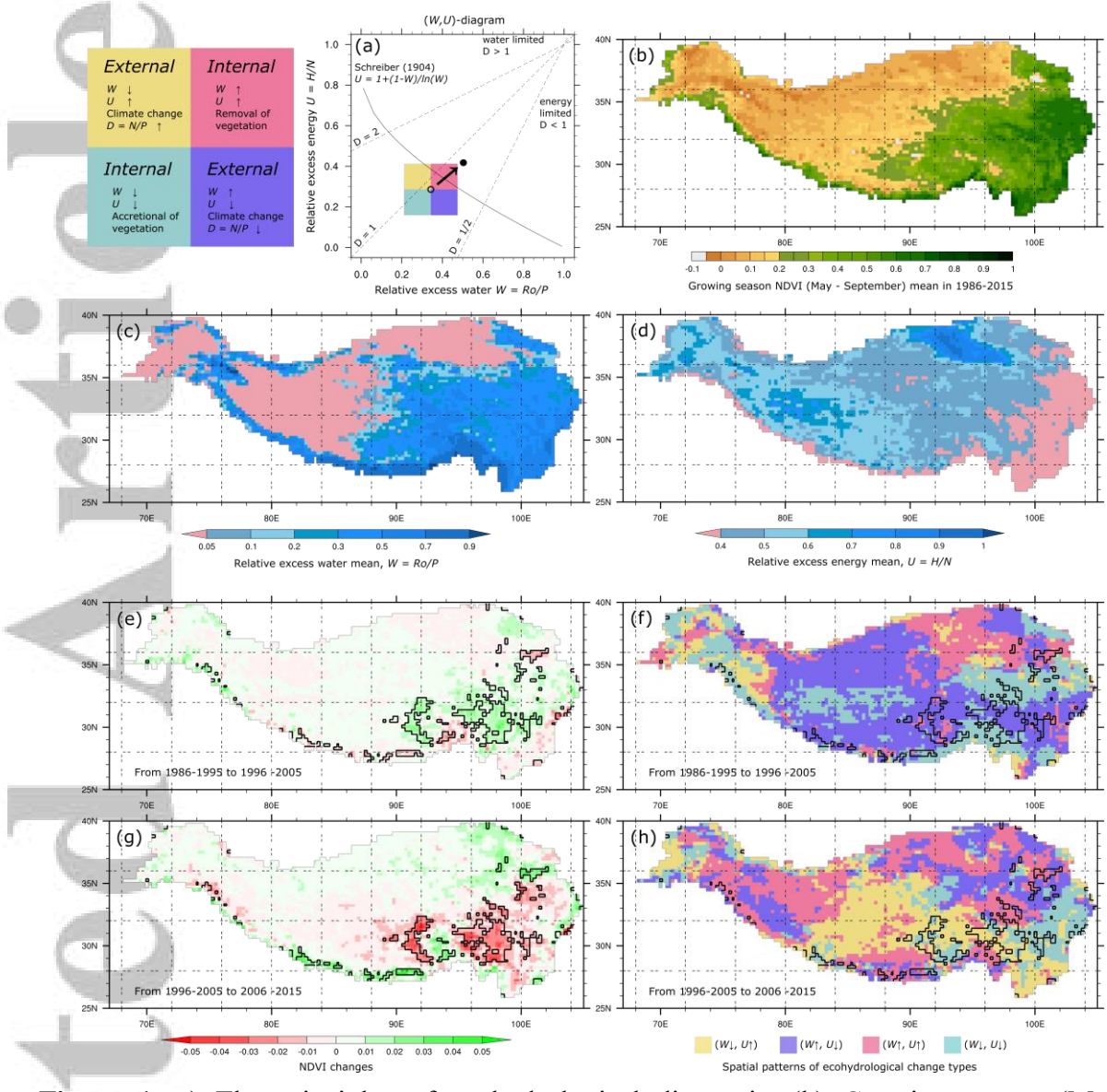

Figure 1. a) The principles of ecohydrological diagnosis. (b) Growing season (May - September) NDVI mean in 1986-2015; (c) Mean relative excess water *W=Ro/P* ; (d) Mean relative excess energy *U=H/N* ; (e) (g) Growing season NDVI changes among three periods: 1986-1995, 1996-2005, 2006-2015; (f) (h) The classification of eco-hydrological state in the (*W*, *U*) diagram, in which the type of change can be expressed as the direction of trajectory; Areas included in black bounds are where there is inconsistent NDVI change between the two periods as defined by $|C_{S1} - C_{S2}| > 0.03$, where C_{S1} and C_{S2} are the changes of NDVI value in Stage 1 (from 1986-1995 to 1996-2005) and Stage 2 (from 1996-2005 to 2006-2015), respectively.

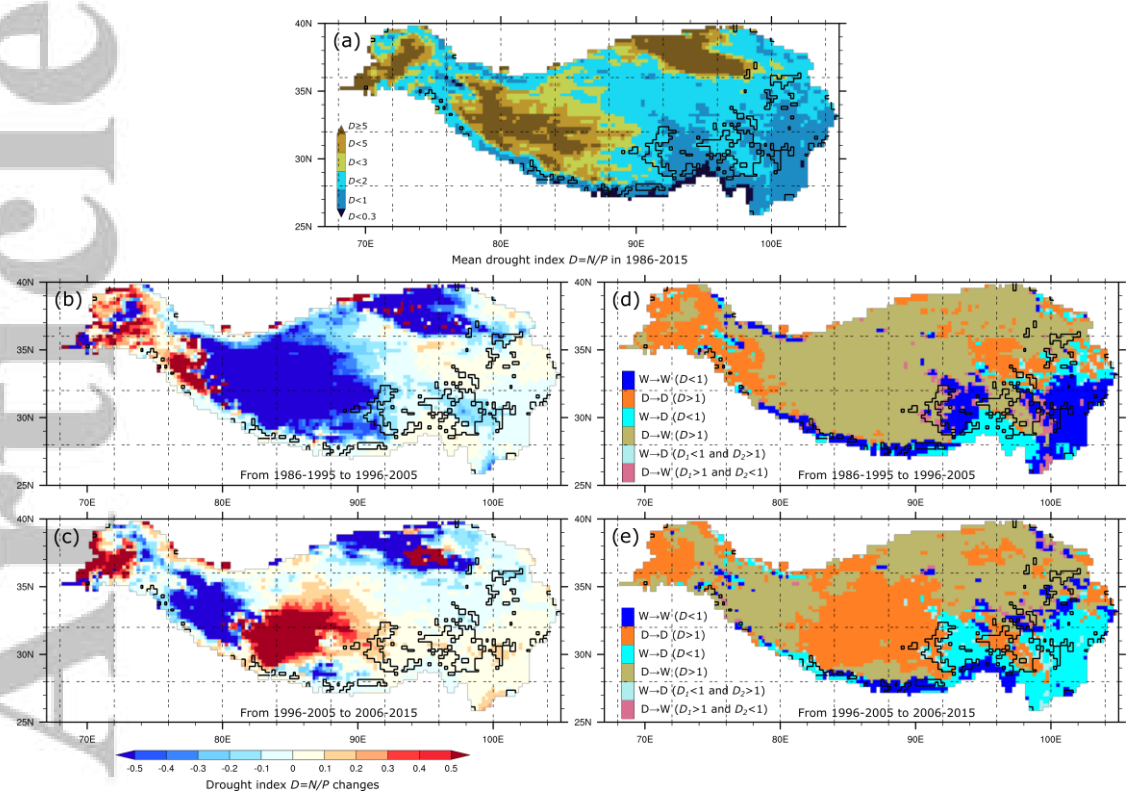

Figure 2. Spatial patterns of drought index: climatology, change and changing types. (a) Mean drought index $D=N/P$ in 1986-2015; (b) (c) Drought index changes over the two stages (stage 1: 1986-1995 to 1996-2005, stage 2: 1996-2005 to 2006-2015); (d) (e) Spatial patterns of drought index change types in the corresponding stages. The threshold of wet vs dry status is defined as drought index $D=1$. Legend W→W refers to wet areas get wetter, D→D refers to dry areas get drier. Legend W→D ($D<1$) refers to wet areas becoming drier but remaining as $D<1$ and vice versa. Legend W→D ($D_1<1$ and $D_2>1$) refers to wet areas turning into dry areas through crossing the threshold $D=1$ and vice versa.

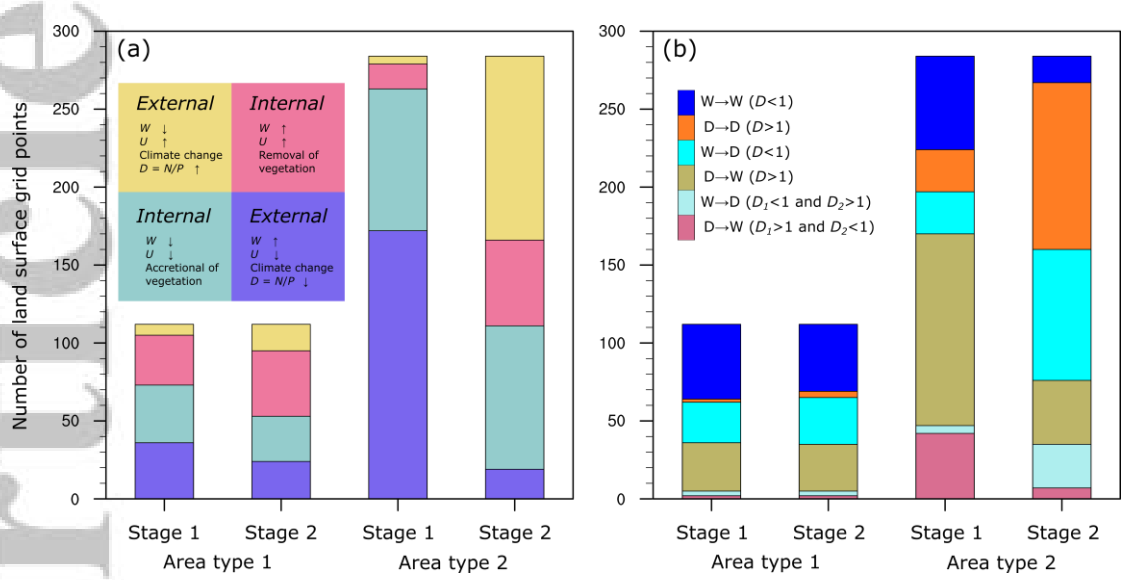

Figure 3. Number of land surface grid points within T1 and T2 showing each of (a) the four eco-hydrological diagnostic status classes and (b) the six drought change types.. Areas included in black bounds (Figure 1e, f) are separated into two types: area type 1 (T1) shows NDVI decrease in Stage 1 (1986-1995 to 1996-2005) and increase in Stage 2 (1996-2005 to 2006-2015). Area type 2 (T2) shows the opposing NDVI change (increase in Stage 1 and decrease in Stage 2).

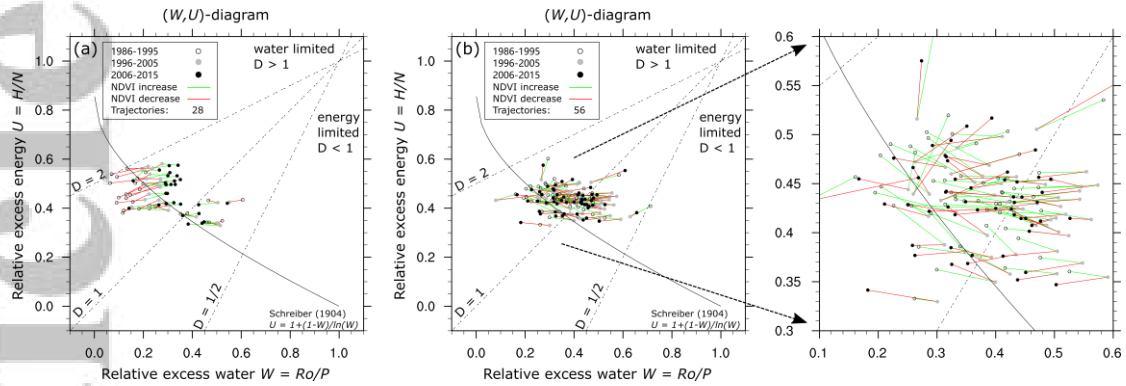

Figure 4. Ecohydrological change diagrams. (a) Trajectories of excess water and energy changes in area type 1. (b) Trajectories of excess water and energy changes in area type 2. The trajectories in both area types are filtered. In area type 1, trajectories with differences below 0.05 in *W* and *U* in Stage 1 and Stage 2 are eliminated. In area type 2, trajectories with differences below 0.08 in *W* and *U* in Stage 1 and Stage 2 are eliminated. Thus, all displayed trajectories are significant in at least one variable with one changing stage. To the right of panel b) magnification makes the trajectories easier to see.